

Translational diffusion of water and its dependence on temperature in charged and uncharged clays: A neutron scattering study

Fátima González Sánchez, Fanni Jurányi, Thomas Gimmi, Luc Van Loon, Tobias Unruh, and Larryn W. Diamond

Citation: *The Journal of Chemical Physics* **129**, 174706 (2008); doi: 10.1063/1.3000638

View online: <http://dx.doi.org/10.1063/1.3000638>

View Table of Contents: <http://scitation.aip.org/content/aip/journal/jcp/129/17?ver=pdfcov>

Published by the [AIP Publishing](#)

Articles you may be interested in

[Diffusion of water in bentonite clay: Neutron scattering study](#)

AIP Conf. Proc. **1512**, 918 (2013); 10.1063/1.4791339

[Structural changes of poly\(N -isopropylacrylamide\)-based microgels induced by hydrostatic pressure and temperature studied by small angle neutron scattering](#)

J. Chem. Phys. **133**, 034901 (2010); 10.1063/1.3447386

[Dynamical changes of hemoglobin and its surrounding water during thermal denaturation as studied by quasielastic neutron scattering and temperature modulated differential scanning calorimetry](#)

J. Chem. Phys. **128**, 245104 (2008); 10.1063/1.2943199

[Single-particle dynamics in dimethyl–sulfoxide/water eutectic mixture by neutron scattering](#)

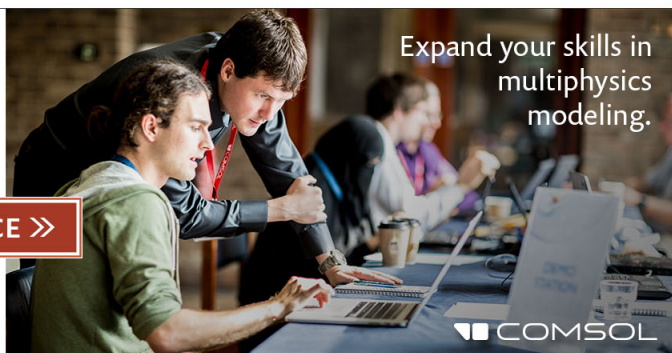
J. Chem. Phys. **113**, 8736 (2000); 10.1063/1.1315333

[X-ray and neutron scattering studies of the temperature and pressure dependence of the structure of liquid formamide](#)

J. Chem. Phys. **106**, 7913 (1997); 10.1063/1.473805

Ready, set, simulate.

REGISTER FOR THE COMSOL CONFERENCE >>



Translational diffusion of water and its dependence on temperature in charged and uncharged clays: A neutron scattering study

Fátima González Sánchez,^{1,a)} Fanni Jurányi,² Thomas Gimmi,^{1,3} Luc Van Loon,¹ Tobias Unruh,⁴ and Larry W. Diamond³

¹Laboratory for Waste Management, Paul Scherrer Institut, CH-5232 Villigen PSI, Switzerland

²Laboratory for Neutron Scattering, Paul Scherrer Institut, CH-5232 Villigen PSI, Switzerland

³Institute of Geological Sciences, University of Bern, CH-3012 Bern, Switzerland

⁴Forschungsneutronenquelle Heinz Maier-Leibnitz (FRM II), 85747 Garching, Germany

(Received 11 April 2008; accepted 23 September 2008; published online 6 November 2008)

The water diffusion in four different, highly compacted clays [montmorillonite in the Na- and Ca-forms, illite in the Na- and Ca-forms, kaolinite, and pyrophyllite (bulk dry density $\rho_b = 1.85 \pm 0.05 \text{ g/cm}^3$)] was studied at the atomic level by means of quasielastic neutron scattering. The experiments were performed on two time-of-flight spectrometers and at three different energy resolutions [FOCUS at SINQ, PSI (3.65 and 5.75 Å), and TOFTOF at FRM II (10 Å)] for reliable data analysis and at temperatures between 27 and 95 °C. Two different jump diffusion models were used to describe the translational motion. Both models describe the data equally well and give the following ranking of diffusion coefficients: Na-montmorillonite \leq Ca-montmorillonite $<$ Ca-illite $<$ Na-illite $<$ water \leq pyrophyllite \leq kaolinite. Uncharged clays had slightly larger diffusion coefficients than that of bulk water due to their hydrophobic surfaces. The time between jumps, τ_j , follows the sequence: Ca-montmorillonite \geq Na-montmorillonite $>$ Ca-illite $>$ Na-illite \geq kaolinite $>$ pyrophyllite \geq water, in both jump diffusion models. For clays with a permanent layer charge (montmorillonite and illite) a reduction in the water content by a factor of 2 resulted in a decrease in the self-diffusion coefficients and an increase in the time between jumps as compared to the full saturation. The uncharged clay kaolinite exhibited no change in the water mobility between the two hydration states. The rotational relaxation time of water was affected by the charged clay surfaces, especially in the case of montmorillonite; the uncharged clays presented a waterlike behavior. The activation energies for translational diffusion were calculated from the Arrhenius law, which adequately describes the systems in the studied temperature range. Na- and Ca-montmorillonite ($\sim 11\text{--}12 \text{ kJ/mol}$), Na-illite ($\sim 13 \text{ kJ/mol}$), kaolinite and pyrophyllite ($\sim 14 \text{ kJ/mol}$), and Ca-illite ($\sim 15 \text{ kJ/mol}$) all had lower activation energies than bulk water ($\sim 17 \text{ kJ/mol}$ in this study). This may originate from the reduced number and strength of the H-bonds between water and the clay surfaces, or ions, as compared to those in bulk water. Our comparative study suggests that the compensating cations in swelling clays have only a minor effect on the water diffusion rates at these high densities, whereas these cations influence the water motion in non-swelling clays. © 2008 American Institute of Physics. [DOI: 10.1063/1.3000638]

I. INTRODUCTION

The behavior of water in confinement has been extensively studied in different environments such as biological cells, at the surface of proteins and membranes, and in clays.^{1,2} Argillaceous rocks and compacted clays are being considered worldwide as barriers for the deep geological disposal of radioactive waste. The study of the dynamics of water confined in clay minerals is important for the understanding of the properties of water within and the transport mechanisms of dissolved components through clays, and thus of the fate of radioactive contaminants.

Clay minerals are aluminum phyllosilicates with a layered structure. They are composed of tetrahedral (*T*: silicon tetrahedra) and octahedral (*O*: aluminum octahedra) sheets. Two or three such sheets form a *TO* or *TOT* layer. Several

sequences of these layers are combined to form larger units called stacks, which again can cluster into particles or aggregates. Substitution of one cation for another without change in the structure (isomorphic substitution), either in the tetrahedral or octahedral layer, can result in a net negative charge. These charges are compensated by interlayer cations and cations on or near the external surfaces. The state of water in clays depends on the type of clay (charged or uncharged) and the degree of compaction and hydration. The clays used in this article for the study of the dynamics of water at the microscopic scale were selected because of their different structures and way of hydrating. The charged clays montmorillonite (swelling) and illite (non-swelling) have a *TOT* structure and were saturated with Na and Ca cations. In montmorillonite, water is located in between particles and in the interlayer space. In illite, however, water is located only in between particles because the interlayer surfaces are tightly linked by potassium cations. The uncharged clays

^aElectronic mail: fatima_oti@yahoo.com.

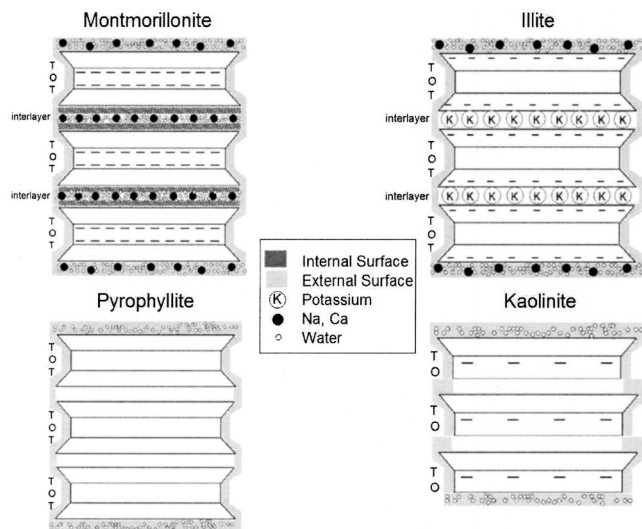


FIG. 1. Schematic representation of the structures of the clays used. The small horizontal lines represent the negative charges of the clay structure. Kaolinite has a very small permanent charge with a CEC of 3.3 milliequivalents/100 g (after Ref. 31).

(non-swelling) studied were pyrophyllite (*TOT* structure) and kaolinite (*TO* structure). They have no interlayers because their primary sheets are not (pyrophyllite) or only very weakly (kaolinite) charged. Therefore, only the external surfaces are hydrated (see Fig. 1).

The particular layered configuration of smectites (swelling clay type) makes them very attractive for the study of the structure and dynamics of water in confinement. The dynamics of water in smectites was extensively studied at the microscopic scale by means of molecular modeling,^{3,4} as well as by various experimental techniques covering a broad range of time scales, such as neutron scattering (from a few picoseconds⁵ to a few nanoseconds⁶) and nuclear magnetic resonance studies⁷ (a few microseconds). Most experiments on swelling clays were performed with clay pastes or powders, and in fact, NMR investigations are in general only possible at rather low bulk dry densities.⁸ Little is known, in contrast, about compacted clays, which are favored artificial sealing materials for radioactive waste. A high compaction of the clays reduces the interparticle pore size⁹ and therefore may affect the water-clay interaction. Some of the early quasielastic neutron scattering (QENS) work^{10,11} as well as more recent work^{12,13} focused on mono- and bihydrated (i.e., containing on the average one or two layers of water between surfaces) swelling clays. The results are, however, not completely conclusive, as outlined by Malikova *et al.*,¹² which is possibly also connected to the different resolutions achieved. Some of the early QENS work as well as more recent work focused on mono- and bihydrated (i.e., containing on the average one or two layers of water between surfaces) swelling clays. The results connected to the different resolutions that were achieved as well. Also, the cations within the clays play an important role in clay swelling as well as in the motion of water depending on their hydration properties¹⁴ and their location within the clay structure.¹⁵ Malikova *et al.*¹⁶ performed a complete theoretical (molecular modeling) and experimental study (neutron time of flight

and spin echo) on the dynamics of water in Cs- and Na-montmorillonite at different hydrations. These three different techniques reached similar values for the water diffusion in a two-layer hydrated Na-montmorillonite at a room temperature of $D=(5-10)\times 10^{-10}$ m²/s. Slightly larger values of D between 11.3 and 12.4×10^{-10} m²/s were found in an earlier study for Ca-montmorillonite at the same hydration (two layer) with neutron time-of-flight techniques.¹¹ In these clays water mobility is reduced with decreasing hydration, as shown experimentally and by molecular modeling,¹⁶ while the residence time, jump length, and rotational relaxation times of the water molecules increase.¹⁷

The main novelty of this article is the study of non-swelling clays such as illite, kaolinite, or pyrophyllite. These clays have received less attention regarding water dynamics. According to our knowledge, there is no neutron scattering study on the dynamics of water in such clays nor a comparative study in highly compacted charged and uncharged clays with different cation saturations. Pyrophyllite and kaolinite have a more hydrophobic character,^{18,19} in contrast to montmorillonite or illite. In molecular modeling studies, hydrophobic surfaces were found to increase water diffusion coefficients as compared to that of bulk water.²⁰⁻²² On the other hand, molecular dynamics simulations²³ of the water motion in kaolinite at room temperature showed diffusion coefficients at the kaolinite interface of $D=9.6\times 10^{-11}$ m²/s. This value corresponds to the average of the *T* and *O* sides, where the tetrahedral side is hydrophobic whereas the octahedral side is hydrophilic.^{24,25} At present, we are not aware of any experimental study that confirms one or the other modeling result in clay samples.

Temperature is an important factor for the performance assessment of radioactive waste repositories. The retention properties of the clays have to persist over a certain range of elevated temperatures due to the heat produced by the decay of radionuclides. Temperature also affects significantly the diffusion of water or solutes. From the temperature dependence of diffusion, the activation energy for diffusion can be derived and vice versa. This dependency usually follows the empirical Arrhenius equation

$$D = Ae^{-E_a/RT}, \quad (1)$$

where D is the diffusion coefficient, A is the pre-exponential factor, $R=8.314$ J/K mol is the molar gas constant, and E_a is the activation energy. The translational residence time also follows the Arrhenius equation.

In charged clays we expect that the compensating cations and the clay surfaces influence the activation energy as compared with bulk water. Ions can be divided into two groups: kosmotropes (order makers: Mg²⁺, Ca²⁺, Li⁺, Na⁺, H⁺) and chaotropes (disorder makers: K⁺, Rb⁺, Cs⁺, Br⁻, I⁻).²⁶ The members of the first group exhibit stronger interactions with water molecules than water with itself, which in aqueous solutions results in a slow down of the water diffusion²⁷ and in an increase in the water E_a .²⁶ Experimental and theoretical studies^{11,28} about the effect of temperature on the dynamics of water in smectites showed activation energies close to or lower than that of bulk water (~ 18 kJ/mol), in contrast to the effect created by cations in solution.

TABLE I. Characterization of clay pellets that are full-, half- and quarter-hydrated (f.h, h.h and q.h respectively). The gravimetric water content is expressed as grams of water per grams of dry clay.

	d spacing (Å)	No. of water molecules/cation	Water (g/g)	Water layers
Na-montmorillonite f.h/h.h/q.h	14.79/11.35/11.06	8–9/4–5/2–3	$(0.16/0.80/0.040) \pm 0.001$	$\approx 2/1/0.5$
Ca-montmorillonite f.h/h.h	15.82/15.17	16–18/8–9	$(0.15/0.075) \pm 0.001$	$\approx 2/1$
Na-illite f.h/h.h	9.92/9.90	30/15	$(0.14/0.070) \pm 0.001$	$\approx 9/4$
Ca-illite f.h/h.h	10.11/10.11	60/30	$(0.15/0.075) \pm 0.001$	$\approx 9/4$
Kaolinite f.h/h.h	7.16/7.16	...	$(0.13/0.065) \pm 0.001$	$\approx 20/10$
Pyrophyllite ^a h.h	9.2	...	$(0.075) \pm 0.001$	≈ 60

^aPyrophyllite was only h.h: a full saturation was not possible due to its strong hydrophobic character.

In this article, we present the properties of the diffusion of water at a microscopic scale obtained with QENS for charged and uncharged clays. These clays were compacted to a high dry density of $\rho_b = 1.85 \pm 0.05$ g/cm³ and investigated at temperatures between 27 and 95 °C to derive activation energies. For some clays the hydration was further reduced to test whether the water mobility can be related or not to the fraction of the different water types.

II. MATERIALS

The clays used in this study were montmorillonite from Milos,²⁹ illite from du Puy,³⁰ kaolinite from Georgia [KGa-2 (Ref. 31)], and pyrophyllite from North Carolina (Ward Natural Science 46E4630). For the neutron scattering measurements, pellets ($5 \times 1.5 \times 0.1$ cm³) with a bulk dry density of $\rho_b = 1.85 \pm 0.05$ g/cm³ were pressed from the powder hydrated with the desired amount of water and encapsulated in a tight aluminum sample holder. Half-hydrated (h.h) samples were obtained from the fully-hydrated (f.h) ones by letting them dry at room temperature. They were encapsulated again and measured one or two days later only to obtain hydration equilibrium. Once the samples were measured in a f.h or h.h state they were dehydrated at 110 °C for 24 h and measured again in the neutron spectrometer.

Several techniques were used to characterize the clay powders and pellets as described in detail by González Sánchez *et al.*³² The different characteristics of the f.h and h.h clay pellets are presented in Table I. The average number of water molecules per cation (for the charged clays) were calculated from the cation exchange capacity (CEC) and the gravimetric water content of the clays. For montmorillonite the CEC used was 99 milliequivalents/100 g,³³ and for illite, it was 26.6 milliequivalents/100 g.³¹ The last column in Table I shows the average number of water layers between two clay surfaces calculated as given by González Sánchez *et al.*³² for Na- and Ca-montmorillonite, Na- and Ca-illite, and kaolinite. Pyrophyllite (with 30% porosity) was calculated in the same way using an S_{BET} (external surface area) of 6.93 m²/g, considering $S_{\text{BET}} \approx S_{\text{EGME}}$ (total surface area) as stated by Scheidegger *et al.*³⁴ For montmorillonite in the f.h form we have an average of about two layers of water between the surfaces, in the h.h about a single layer, and in the quarter-hydrated (q.h) statistically half a water layer (see Table I). These numbers agree well with x-ray diffraction measurements because of the stepwise change in the d

spacing.³⁵ Similar samples at similar densities have approximately 100% of the total water in the interlayers³⁶ which can be assumed also in our case.

The particle alignment of the compacted pellets was probed by x-ray and neutron texture goniometry³⁷ experiments. The pellets were found to be mainly randomly oriented.

III. METHODS

QENS experiments were carried out at SINQ, Paul Scherrer Institut in Villigen, Switzerland, on the hybrid time-of-flight spectrometer FOCUS (Ref. 38), and at the FRM II in Garching, Germany, on the chopper time-of-flight instrument TOFTOF.³⁹ Three wavelengths were selected to better determine the parameters of the translational and rotational motions. The experimental settings for the three incident wavelengths (λ_i) are summarized in Table II. The sample was encapsulated in a watertight rectangular aluminum sample holder and placed at a 45° slab angle (transmission) into the beam. The measurements were performed at temperatures ranging from 27 to 95 °C. Vanadium was used for detector efficiency calibration and to determine the energy resolution of the instruments. No broadening of the elastic line was found for the dry samples; the obtained line shapes were identical to the resolution function. The spectra of the dry samples and the empty sample holder were used to account for the background. Bulk water was measured as a reference at the FOCUS spectrometer at 5.75 Å.

QENS in clay-water systems is dominated by the incoherent cross section of the hydrogen. The hydrogen dynamics is assumed to represent the dynamics of the water molecules in these systems. The data as a function of Q (momentum transfer) and $\hbar\omega$ (energy transfer) were fitted by the following expression:

$$I(Q, \omega) = \{A(Q) \cdot \delta(E) + B(Q) \cdot S(Q, \omega)\} \otimes G(Q, \omega) + C(Q), \quad (2)$$

with $A(Q) \cdot \delta(E)$ a contribution of the elastic scattering origi-

TABLE II. Experimental settings for the three wavelengths used.

Instrument	λ_i (Å)	δE (μeV)	Q range (Å^{-1})	Measured T (°C)
FOCUS	3.65	250	0.36–2.65	27
FOCUS	5.75	45	0.26–1.65	27,35,45,60,70,95
TOFTOF	10	13	0.22–1.12	27,45,95

nating from the dry clay, $S(Q, \omega)$ a model quasielastic scattering function of water, $B(Q)$ the intensity of the diffusing water, $G(Q, \omega)$ the Gaussian-like spectrometer resolution function, and $C(Q)$ a constant background. Using the approximation that the rotational and translational motions of the water are independent, the scattering function $S(Q, \omega)$ can be written by the convolution of the rotational and translational components in the following manner:

$$S(Q, \omega) \approx S_{\text{inc}}(Q, \omega) \approx S_{\text{trans}}(Q, \omega) \otimes S_{\text{rot}}(Q, \omega). \quad (3)$$

This approximation has been found to be valid for bulk water in the low Q range,⁴⁰ which is the range used to obtain the translational diffusion coefficients.

In clays, water may be present in interlayers, on external layers, and as free pore water, with varying ratios depending on the type of clay. Accordingly, the motion of the water molecules observed by QENS must be regarded as an average of the different water types, weighted by their corresponding fractions. We assumed that, at the given time resolutions, the translational diffusion can be described by a three dimensional (3D), random, and spatially isotropic motion. In this model the incoherent scattering can be described by a Lorentzian function:⁴¹

$$S_{\text{trans}}(Q, \omega) = \frac{1}{\pi} \frac{\Gamma_i(Q)}{\omega^2 + \Gamma_i^2(Q)}, \quad (4)$$

where $\Gamma_i(Q)$ is the half width at half maximum of the Lorentzian curve and depends on the parameters of the diffusive motion. At low momentum transfers, $\Gamma_i(Q)$ can be approximated by the continuous diffusion model (Fick's law), where $\Gamma_i(Q) = \hbar D Q^2$: $\hbar = 0.658$ meV·ps is the reduced Planck constant and D the diffusion coefficient. At large momentum transfers Fick's law is no longer applicable because the diffusion process at atomistic scales becomes important. This behavior is described by the widely used jump diffusion models, in which the atom or molecule spends a considerable time (τ_j) at a quasiequilibrium position before it rapidly jumps to the next quasiequilibrium position.⁴² The data $\Gamma_i(Q)$ shown here were fitted by the Singwi–Sjölander⁴³ and the Hall–Ross⁴² model. Both models have been successfully used to describe water dynamics in clay minerals^{17,44} but may lead to slightly different parameters. Thus, the assumption of a specific model can result in a systematic error. We applied the two different models to have an estimate of this error. The difference between them is that they rely on two different distribution functions for the jump lengths but both converge to the Fickian limit for low Q . The Singwi–Sjölander model is based on an exponential distribution of jump lengths and leads to

$$\Gamma_i(Q) = \frac{\hbar D_{\text{SS}} Q^2}{1 + D_{\text{SS}} Q^2 \tau_{i,\text{SS}}}. \quad (5)$$

The Hall–Ross model assumes a Gaussian distribution of jump lengths, which results in

$$\Gamma_i(Q) = \frac{\hbar}{\tau_{i,\text{HR}}} [1 - \exp(-Q^2 D_{\text{HR}} \tau_{i,\text{HR}})]. \quad (6)$$

The mean jump length for the two models is defined by

$$l = \sqrt{6D\tau_i}. \quad (7)$$

The rotation of the water molecules is assumed to be continuous and isotropic and can be expressed by the well known Sears expansion:⁴⁵

$$S_{\text{rot}}(Q, \omega) = j_0^2(Qa) \delta(E) + \frac{1}{\pi} \sum_{n=1}^3 (2n+1) \times j_n^2(Qa) \frac{n(n+1)(\hbar/6\tau_r)}{\omega^2 + (n(n+1)(\hbar/6\tau_r))^2}. \quad (8)$$

The term $\delta(E)$ is the Dirac delta function, j_n are the spherical Bessel functions, $a = 0.98$ Å is the O–H distance of the water molecule, and τ_r is the rotational relaxation time. In our measurement Q was limited to a maximum of 2.65 Å⁻¹; therefore the terms for $n > 3$ in Eq. (8) could be neglected. Equations (2)–(8) were fitted to the measured $S(Q, \omega)$ to obtain the translational diffusion coefficients, residence times, and rotational relaxation times for water at different temperatures and different hydration states of the samples.

The assumption of a translational diffusion described by a locally 3D, random, and spatially isotropic motion is realistic for clays such as illite (Na- and Ca-), kaolinite, and pyrophyllite with a large average number of water layers in their structure (see Table I). However, for Na- and Ca-montmorillonite it might not be entirely correct. The montmorillonite clay with two water layers has almost all the water molecules in the interlayer space which can be considered as a two dimensional (2D) confinement. Thus the spectra of montmorillonite samples were analyzed additionally with a 2D dynamical model for randomly oriented particles,^{41,46} which is discussed in Sec. IV D.

IV. RESULTS AND DISCUSSION

The quality of the fits is shown in Fig. 2 for kaolinite at the three different wavelengths. The values calculated for the three wavelengths were in good agreement for all clays and at all the different hydrations and temperatures. Accordingly, we treated the data $\Gamma_i(Q)$ obtained at the different wavelengths as a single set to estimate D and τ_r . An example of $\Gamma_i(Q)$ for different λ_i is shown in Fig. 3 for f.h Na-illite and h.h Ca-illite. In contrast, the choice of the jump diffusion model had a significant influence on the estimated parameters. The diffusion coefficients were always 10–20% larger for the Singwi–Sjölander than for the Hall–Ross model (see Table III), the time between jumps 10%–20% smaller for all the data analyzed (see Table IV). Because the fits were equally good for both models, we cannot decide which model characterizes the data better (see the quality of the fits in Fig. 4). The systematic error introduced by the model can be observed by comparing both results. It may be possible that a different jump length distribution applies for charged clays at high bulk densities (low water contents) as compared to bulk water. Accordingly, for charged clays average values may be used and the systematic uncertainty should be considered for relative comparisons, not just for absolute values.

At low values of Q (where D is obtained) the quasielastic scattering is mainly caused by translational displacement

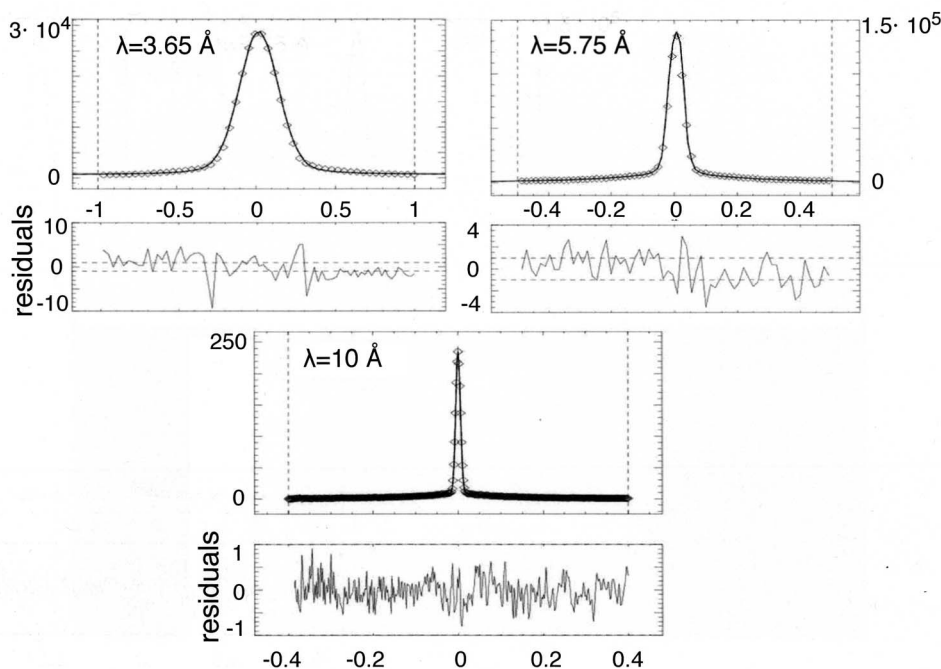


FIG. 2. Typical fits of the QENS spectra. Intensity (arbitrary units) vs energy exchange (meV) for kaolinite at $Q \sim 1 \text{ \AA}^{-1}$ and $T = 27 \text{ }^\circ\text{C}$.

motions and the rotational contribution is almost negligible. However, at high Q values (where τ_r is obtained), both rotation and translation contribute significantly to the quasielastic scattering. Thus the obtained τ_r is generally considered to be less reliable than the D values.

A. Translational diffusion parameters for fully hydrated samples at 300 K

The data obtained (see Table III) for bulk water are in good agreement with other neutron scattering data^{11,47} as well as other measurements.⁴⁸ In summary, the diffusion coefficients obtained for the charged clays were strongly reduced, whereas those for the uncharged kaolinite were identical or slightly higher compared to those for bulk water (see Table III). The diffusion coefficients at 300 K (as generally all temperatures) followed the following increasing order: Na-montmorillonite \approx Ca-montmorillonite $<$ Ca-illite $<$ Na-illite $<$ water \leq kaolinite. The residence time (see Table IV) and mean jump length followed just the opposite order, the values of kaolinite in this case being larger than those of bulk water. Within the context of the jump diffusion model, the slower diffusion as compared to that of the bulk water is mainly caused by the longer residence time, which is only partly compensated by the larger jump length. The jump lengths can be directly extracted from Tables III and IV. For comparative reasons, the approximate values between the two models are given here: water $\sim 1.5 \text{ \AA}$, Na-montmorillonite (f.h) \approx Ca-montmorillonite (f.h) $\sim 2.9 \text{ \AA}$, Na-illite (f.h) $\sim 1.7 \text{ \AA}$, Ca-illite (f.h) $\sim 2.2 \text{ \AA}$, kaolinite (f.h) $\sim 2.0 \text{ \AA}$, and pyrophyllite (h.h) $\sim 1.6 \text{ \AA}$.

For montmorillonite the diffusion coefficients are approximately half of the ones in bulk water, the residence time eight times larger, and the jump lengths about two times larger. The type of cation has only a slight effect on the water motion in montmorillonite, whereas in illite it strongly af-

fects the diffusion parameters. Na^+ and Ca^{2+} behave very differently when hydrated.¹⁴ Ca^{2+} has a much higher hydration energy (-1660 kJ/mol) than Na (-440 kJ/mol) and is also more electronegative; therefore the water molecules are much more strongly bound to Ca^{2+} than to Na^+ . Ca-illite had 30% smaller D than the Na-form. Due to the compensating cations, the water dynamics in this type of clay can be compared with that in aqueous solutions of $4M$ NaCl [$D = (1.85 \pm 0.1) \times 10^{-9} \text{ m}^2/\text{s}$ (Ref. 49)] and $2M$ CaCl_2 [$D = (1.40 \pm 0.05) \times 10^{-9} \text{ m}^2/\text{s}$ (Ref. 50)], respectively, where CaCl_2 at half concentration than NaCl (as it happens in the clay structure) reduces stronger the water dynamics. A similar difference in diffusion of water, depending on the saturating cation, was observed in our illite samples. We are not aware of any other measurement of the local water diffusion coefficients in illites.

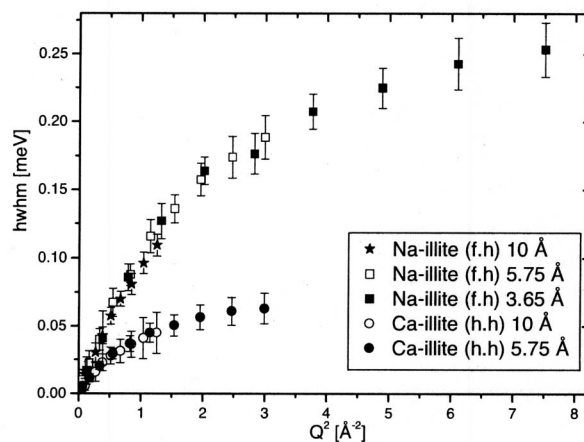


FIG. 3. The translational diffusion broadening Γ_l (meV) vs Q^2 (\AA^{-2}) for the three incident wavelengths ($\lambda_i = 3.65, 5.75,$ and 10 \AA) for f.h Na-illite and h.h Ca-illite.

TABLE III. Values for the diffusion coefficient D (m^2/s) for bulk water and f.h, h.h, and q.h clays. obtained by the two jump diffusion models (SS: Singwi–Sjölander and HR: Hall–Ross). The abbreviations correspond to Na-montmorillonite (Na-m), Ca-montmorillonite (Ca-m), Na-illite (Na-i), Ca-illite (Ca-i), kaolinite (Kao), and pyrophyllite (Pyro).

D (10^{-9} m^2/s)	27 °C		35 °C		45 °C	
	SS	HR	SS	HR	SS	HR
Water	2.37 ± 0.08	2.30 ± 0.10	$(2.84 \pm 0.26)^a$	$(2.75 \pm 0.26)^a$	3.73 ± 0.20	3.58 ± 0.12
Na-m (f.h)	1.21 ± 0.12	0.98 ± 0.05	1.30 ± 0.11	1.08 ± 0.06	1.45 ± 0.10	1.20 ± 0.10
Ca-m (f.h)	1.22 ± 0.08	0.95 ± 0.06	1.33 ± 0.12	1.10 ± 0.12	1.48 ± 0.10	1.22 ± 0.07
Na-i (f.h)	2.15 ± 0.12	1.97 ± 0.10	2.42 ± 0.08	2.27 ± 0.10	2.85 ± 0.11	2.76 ± 0.09
Ca-i (f.h)	1.55 ± 0.10	1.38 ± 0.08	1.90 ± 0.11	1.70 ± 0.08	2.38 ± 0.12	2.15 ± 0.11
Kao (f.h)	2.90 ± 0.16	2.50 ± 0.15	3.76 ± 0.24	3.85 ± 0.18
Pyro (h.h)	2.70 ± 0.10	2.57 ± 0.10	3.83 ± 0.12	3.66 ± 0.16
Na-m (h.h)	0.53 ± 0.09	0.47 ± 0.03	0.78 ± 0.07	0.70 ± 0.05
Na-m (q.h)	0.48 ± 0.04	0.46 ± 0.03
Ca-m (h.h)	0.46 ± 0.03	0.41 ± 0.03
Na-i (h.h)	1.78 ± 0.10	1.62 ± 0.10
Ca-i (h.h)	1.18 ± 0.07	1.08 ± 0.06	1.61 ± 0.12	1.56 ± 0.10
Kao (h.h)	2.81 ± 0.19	2.50 ± 0.12

D (10^{-9} m^2/s)	60 °C		70 °C		95 °C	
	SS	HR	SS	HR	SS	HR
Water	$(4.67 \pm 0.35)^a$	$(4.48 \pm 0.35)^a$	5.87 ± 0.26	5.60 ± 0.12	8.40 ± 0.40	8.00 ± 0.16
Na-m (f.h)	1.86 ± 0.12	1.55 ± 0.06	2.22 ± 0.08	1.81 ± 0.10	2.62 ± 0.20	2.31 ± 0.11
Ca-m (f.h)	1.90 ± 0.14	1.56 ± 0.08	2.09 ± 0.10	1.73 ± 0.10	2.42 ± 0.08	2.23 ± 0.12
Na-i (f.h)	3.60 ± 0.12	3.36 ± 0.08	4.21 ± 0.18	3.92 ± 0.16	5.39 ± 0.25	5.19 ± 0.20
Ca-i (f.h)	2.91 ± 0.16	2.56 ± 0.12	3.38 ± 0.16	3.00 ± 0.12	4.95 ± 0.18	4.44 ± 0.17
Kao (f.h)	6.12 ± 0.24	5.55 ± 0.22	7.80 ± 0.52	7.21 ± 0.43
Pyro (h.h)	5.64 ± 0.20	5.36 ± 0.23	7.89 ± 0.80	7.60 ± 0.33
Ca-i (h.h)	3.20 ± 0.15	3.12 ± 0.18

^aThese values were not measured but obtained for comparison purposes from the activation energy curves [Eq. (1)].

However, in montmorillonite the forces exerted by surfaces and interfaces on water molecules may hinder the full hydration of the cations, and possibly the direct influence of the surfaces masks the cation effect. Previous studies^{20,51} confirmed that the range of influence of the clay surfaces extends to about the first two water layers. Hence all water in our montmorillonite samples was strongly affected by the surfaces.

Our results for the bihydrated Na- and Ca-montmorillonite at room temperature are consistent with other QENS measurements of clay powders.^{11,16} Thus, it seems that just the hydration state but not the sample form (pellets or powder) dominates the local diffusion properties. This is possibly true only for clays with interlayer hydration (smectites).

For kaolinite the diffusion coefficients at 300 K are slightly larger than those measured for bulk water (see Table III). This seems to support those results of molecular modeling studies that reported larger diffusion coefficients on kaolinite surfaces because of the partial hydrophobicity.²⁰⁻²³ However, in view of the small differences in diffusion coefficients and possible additional uncertainties that arise from the choice of the models for the analysis of the QENS data, the present data set does not allow to make a definite conclusion. Furthermore, considering the fact that our data represent an average over the about 20 water layers between the

kaolinite surfaces, with both hydrophilic and hydrophobic surfaces present, the hydrophobic surfaces must either affect the first few water layers very strongly or otherwise have a very long range of influence.

B. Translational diffusion parameters for half-hydrated samples at 300 K

The results for the partially hydrated samples are presented in Tables III and IV. The dehydration produced a significant effect in the diffusion parameters of the charged clays (lower diffusion coefficients) but no variation in the case of kaolinite.

Kaolinite at the reduced water content has similar diffusion parameters as in the f.h state, with a diffusion coefficient still only slightly larger than that of bulk water. This contradicts the interpretation that hydrophobic surfaces that affect strongly the first few water layers only are responsible for the increase in the observed D ; in this case, an increased effect at the lower water content would have been expected. The findings may be interpreted in two other ways. One is that the hydrophobic surfaces indeed lead to the larger D but they affect many and not just the first few water layers. Then, a reduction in the water content (from 20 to 10 layers between surfaces) would not increase the effect. Alternatively, kaolinite at the reduced water content may still have mostly free

TABLE IV. Values for the residence time τ_r (ps) for bulk water and f.h, h.h, q.h clays obtained by the two jump diffusion models (SS: Singwi–Sjölander and HR: Hall–Ross).

τ_r (ps)	27 °C		35 °C		45 °C	
	SS	HR	SS	HR	SS	HR
Water	1.00 ± 0.06	1.57 ± 0.12	(0.88 ± 0.35) ^a	(1.36 ± 0.30) ^a	0.71 ± 0.06	1.13 ± 0.37
Na-m (f.h)	11.89 ± 1.00	13.81 ± 0.62	9.09 ± 0.27	11.74 ± 0.64	8.50 ± 0.24	12.00 ± 0.60
Ca-m (f.h)	11.01 ± 0.92	15.41 ± 0.24	10.02 ± 0.70	12.67 ± 1.00	8.84 ± 0.62	12.17 ± 0.24
Na-i (f.h)	1.96 ± 0.20	2.84 ± 0.20	1.54 ± 0.10	2.35 ± 0.16	1.30 ± 0.08	2.08 ± 0.15
Ca-i (f.h)	4.49 ± 0.30	6.29 ± 0.34	3.42 ± 0.30	4.79 ± 0.38	2.74 ± 0.22	4.42 ± 0.22
Kao (f.h)	2.19 ± 0.11	2.31 ± 0.22	1.44 ± 0.09	2.56 ± 0.09
Pyro (h.h)	1.15 ± 0.09	2.05 ± 0.12	0.90 ± 0.06	1.50 ± 0.09
Na-m (h.h)	21.31 ± 1.00	26.49 ± 1.13	14.69 ± 1.00	21.33 ± 1.00
Na-m (q.h)	19.21 ± 1.13	29.50 ± 0.62
Ca-m (h.h)	23.10 ± 0.83	34.24 ± 0.94
Na-i (h.h)	3.00 ± 0.52	4.06 ± 0.76
Ca-i (h.h)	7.73 ± 0.71	10.91 ± 0.50	4.29 ± 0.80	6.85 ± 0.41
Kao (h.h)	2.12 ± 0.14	2.76 ± 0.12

τ_r (ps)	60 °C		70 °C		95 °C	
	SS	HR	SS	HR	SS	HR
Water	(0.62 ± 0.33) ^a	(0.96 ± 0.34) ^a	0.52 ± 0.08	0.82 ± 0.22	0.42 ± 0.11	0.64 ± 0.08
Na-m (f.h)	6.22 ± 0.21	8.07 ± 0.81	5.76 ± 0.22	7.35 ± 0.43	4.26 ± 0.60	5.74 ± 0.25
Ca-m (f.h)	6.84 ± 0.62	8.74 ± 0.60	5.78 ± 0.40	7.44 ± 0.23	3.99 ± 0.21	6.07 ± 0.22
Na-i (f.h)	1.14 ± 0.08	1.71 ± 0.12	0.97 ± 0.06	1.46 ± 0.08	0.75 ± 0.06	1.15 ± 0.09
Ca-i (f.h)	2.41 ± 0.24	3.33 ± 0.23	1.78 ± 0.14	2.53 ± 0.22	1.36 ± 0.08	2.08 ± 0.08
Kao (f.h)	0.91 ± 0.06	1.31 ± 0.10	0.67 ± 0.05	0.99 ± 0.08
Pyro (h.h)	0.64 ± 0.07	1.00 ± 0.08	0.49 ± 0.04	0.81 ± 0.05
Ca-i (h.h)	2.13 ± 0.11	3.21 ± 0.13

^aThese values were not measured but obtained for comparison purposes from the fit of τ_r as a function of temperature with the Arrhenius equation.

pore water, such that the average properties remain similar as those of bulk water and those of the f.h kaolinite. In this case, the small increase in D as compared to bulk water must be regarded as insignificant. At present, no definitive judgment can be made on this topic.

The strong hydrophobic behavior of pyrophyllite made it impossible to fully saturate it at a bulk dry density of $\sim 1.9 \text{ g/cm}^3$, and only a half-water-saturated sample could

be tested. This sample had also a slightly larger diffusion coefficient than bulk water, similar as the kaolinite samples. Accordingly, the same interpretation as for kaolinite is possible, even though the larger number of water layers between surfaces seems to support more the idea that mostly bulk water is present.

The two forms of montmorillonite showed also at the reduced water contents a similar behavior. In the case of montmorillonite the dehydration led to one-layer hydrate and a reduction in the interlayer spacing, as reported in Table I. Accordingly, water will be even more affected by the cations and clay surfaces than in the case of the f.h samples. In these clays the diffusion coefficients and residence times were reduced and increased, respectively, about 50% as compared with the f.h samples. The mean jump length, however, did not change, which was also observed in other studies with powder Ca-montmorillonite¹⁷ for similar hydration states. Malikova *et al.*¹⁶ found similar values for the diffusion coefficients of Na-montmorillonite powder $[(1-3) \times 10^{-10} \text{ m}^2/\text{s}]$ at the same hydration (one layer). We measured Na-montmorillonite at even lower water contents (denoted as a quarter-water-saturated, corresponding to about a half-layer-hydrate on average). No remarkable differences were found as compared with the h.h sample. This means that the average water properties were about identical in the half- and quarter-saturated-water sample. It is also conceivable that the hydration state was more heterogeneous in the

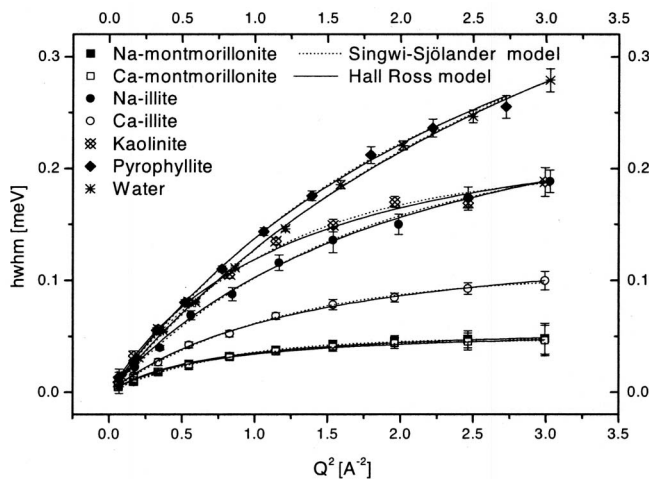


FIG. 4. Fully saturated clays, except h.h pyrophyllite, and water (this study) fitted by the two models, Singwi–Sjölander and Hall–Ross, at $T=27 \text{ °C}$ for $\lambda_i=5.75 \text{ Å}$.

TABLE V. Values for the rotational relaxation time τ_r (ps) for bulk water and fully-, half- and quarter-hydrated (only for Na-montmorillonite) charged clays. The estimated errors are not larger than 5%.

τ_r (ps)	27 °C	35 °C	45 °C	60 °C	70 °C	95 °C
Water	1.08		0.91		0.74	0.61
Na-m (f.h/h/q.h)	1.51/1.69/1.70	1.40/-/-	1.27/1.40/-	1.10/-/-	1.01/-/-	0.86/-/-
Ca-m (f.h/h.h)	1.53/1.67	1.42/-	1.26/-	1.12/-	1.04/-	0.87/-
Na-i (f.h/h.h)	1.10/1.30	0.99/-	0.92/-	0.79/-	0.75/-	0.61/-
Ca-i (f.h/h.h)	1.32/1.52	1.20/-	1.1/1.24	0.97/-	0.88/-	0.74/0.88

case of the half layer hydrate, with some interlayer having still about one water layer, whereas others were completely dried. These results also support the fact that water diffusion in these clays is more affected by the clay surfaces than by the interaction with the cations, as it happened in both illites.

Dehydration in Na- and Ca-illite produced also a reduction in the diffusion parameters but not as pronounced as in montmorillonite. The Ca-form is more affected by dehydration than the Na-form; however, we expect that further reduction in the water content would cause similar water diffusion in both illites, as it happened in Na- and Ca-montmorillonite. Indeed, in the h.h illites with four water layers between the clay particles (see Table I), the diffusion parameters became similar (Ca-illite, $\sim 115\%$) or slightly larger (Na-illite, 140%) than those of f.h Na- and Ca-montmorillonite (bilayer).

C. Rotational diffusion

The rotational relaxation times of water τ_r were comparatively less affected by the clay surfaces and cations than the translational diffusion parameters. Results for the charged clays and bulk water are given in Table V. Uncharged clays had similar values as those of bulk water even at reduced hydrations; therefore they are omitted in the table. The bulk water values were in agreement with the values found in the literature.⁵² Both montmorillonites showed similar τ_r at each temperature and hydration, as it happened with the diffusion coefficients. The τ_r in illite, however, was found to be different for both forms. The Na-form seemed to be closer to the bulk water values, and the Ca-form was more affected by dehydration.

Our measurements are consistent with the data found in literature for one-water-layer hydrated powder of Ca-montmorillonite.¹⁷ Anderson *et al.*¹⁷ found rotational relaxation times twice the value of bulk water. Note that the differences of the rotational relaxation times follow the differences in translational motion: samples with lower diffusion times had generally larger relaxation times.

D. The two-dimensional dynamics

In montmorillonite clays, with one to two water layers, the water motion may be restricted perpendicular to the interlayers and in the extreme case a 2D diffusion of water may result. The time-of-flight measurements presented in this paper have been performed on pressed samples with a given degree of compaction. In these samples there is a

slightly preferred orientation of the particles perpendicular to the press direction; however, the angular distribution is very broad.

Because the quality of the fits for the montmorillonite spectra was not as good as for the other clays, especially at low Q values (see Fig. 5), we fitted the Na-montmorillonite data with a model⁴⁶ that assumes a 3D rotational and a 2D translational motion, with a Gaussian jump length distribution and an isotropic particle arrangement. The quality of the fits obtained for montmorillonite is shown in Fig. 5. The 2D and 3D models had similar quality, being slightly better at high Q than at low Q . This 2D model has a characteristic logarithmic singularity at zero energy transfer. To observe this singularity the instrument resolution has to be significantly smaller than the width of the quasielastic line.⁵³ We estimate the time scale t needed for the “exploration” of the full interlayer as

$$t \approx \frac{l^2}{2D}, \quad (9)$$

with $l \approx 5 \text{ \AA}$ the interlayer thickness (see Table I) and $D \approx 10^{-9} \text{ m}^2/\text{s}$ the local diffusion coefficient obtained using the 3D model at room temperature. The resulting t is about 100 ps which could just be observed at TOFTOF (observation time in the order of 50 ps) but clearly not at FOCUS (15 and 3 ps). Therefore TOFTOF data for Na-montmorillonite were used to test the applicability of the 2D model. The results showed that at low temperatures (27–45 °C) the 2D diffusion parameters were similar to the ones obtained by the 3D model; however, at high temperatures (95 °C) the diffusion coefficients of the 2D model ($D = 3.20 \times 10^{-9} \text{ m}^2/\text{s}$) were larger than those based on the 3D model. Thus, for the given instrument resolution the 2D movement cannot be resolved at the lower temperatures because the time of observation is too short for the restrictions to become relevant. At 95 °C the line shape deviates already from a typical 3D motion, but at the same time the 2D movements are not fully resolved yet and the 2D values are not reliable either. We can conclude that all results except the one at 95 °C measured at TOFTOF (not used in this article) describe the 3D local motion.

E. Temperature dependence

The mean jump lengths obtained for all the clays are about constant at all the temperatures (as for bulk water). Activation energies were calculated using the Arrhenius equation (1). The results are presented in Table VI and the quality of the fits can be seen in Fig. 6. In our experiments

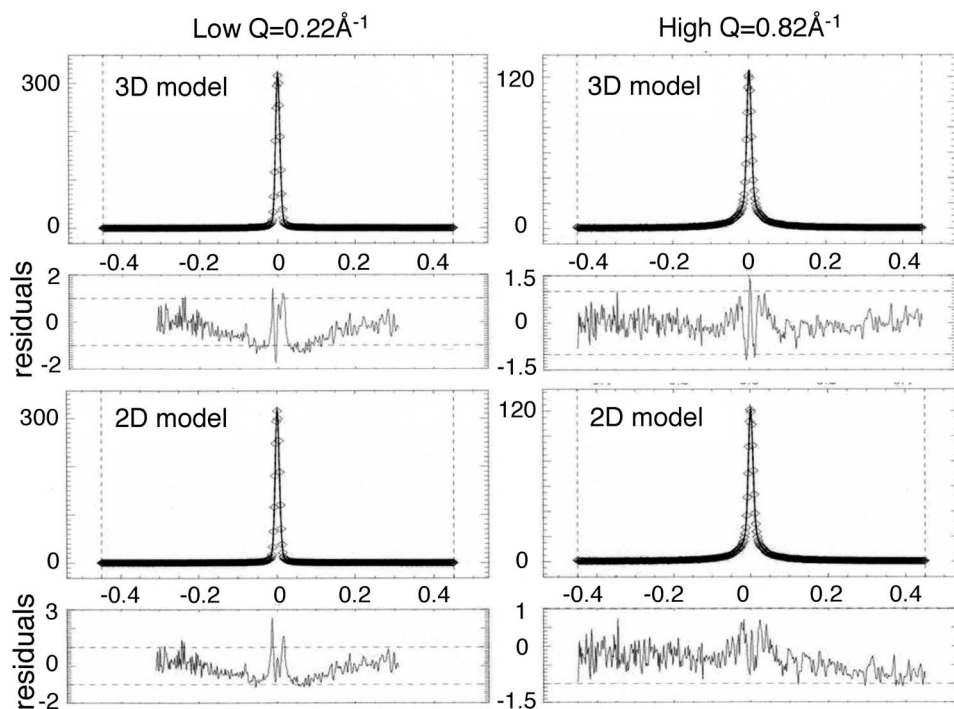


FIG. 5. Intensity (arbitrary units) vs energy exchange (meV) for Na-montmorillonite at $T=27$ °C and $\lambda_j=10$ Å at low $Q=0.22$ Å $^{-1}$ and high $Q=0.82$ Å $^{-1}$ fitted by a 3D and a 2D models.

bulk water had an E_a value of about 17 kJ/mol, which is in agreement with the values found in the literature.^{54,55} Due to the systematic error between the two studied jump diffusion models, the activation energies calculated from both models are almost identical (Table VI). The E_a results for all the clays are between 15 kJ/mol (Ca-illite) and 11–12 kJ/mol (Na- and Ca-montmorillonite). The differences are relatively small (about 30%) despite the large differences in the structure and chemistry of the studied clays. Thus the activation energy of the local diffusive motion is a less sensitive parameter in evaluating the differences of the diffusion in the investigated clays. The E_a values followed the following increasing order: Na-montmorillonite \leq Ca-montmorillonite $<$ Na-illite $<$ kaolinite \leq pyrophyllite $<$ Ca-illite $<$ water. All clays had lower E_a values than that of bulk.

In water solutions it has been observed that the presence of cations (such as Na $^+$ and Ca $^{2+}$) increase the water E_a .²⁶ Therefore one could interpret that, in contrast to the cations, the confinement and close interaction with the surfaces possibly tend to reduce the E_a . The limited space for the water to diffuse and the competition between the cations and clay

surfaces could distort the H-bonds between two water molecules or a water molecule and the clay surfaces or a cation, resulting in a lower E_a . This interpretation is supported by the fact that the jump lengths in montmorillonite are significantly higher than that in bulk water, which means weaker H-bonds. The interpretation seems plausible also in view of the E_a sequence of the studied clays. The clay most affected was montmorillonite, which has the largest geometrical restrictions due to its interlayer structure, followed by Na-illite (less restricted), the uncharged clays (even less restricted), and Ca-illite. In the case of Ca-illite, the weakening of the H-bonds by the surfaces seemed to be compensated by the strong interactions with the Ca cation (stronger kosmotrope

TABLE VI. Values for activation energy E_a (kJ/mol) for bulk water and f.h and h.h clays obtained by the two jump diffusion models (SS: Singwi-Sjölander and HR: Hall-Röss).

E_a (kJ/mol)	SS	HR
Water	16.32 ± 0.70	17.40 ± 0.80
Na-m (f.h)	11.98 ± 1.20	12.16 ± 0.50
Ca-m (f.h)	10.75 ± 0.70	11.42 ± 0.30
Na-i (f.h)	12.76 ± 0.35	12.99 ± 0.30
Ca-i (f.h)	15.10 ± 0.50	15.30 ± 0.56
Kao (f.h)	14.23 ± 1.00	14.54 ± 1.00
Pyro (h.h)	14.50 ± 0.20	14.51 ± 0.20
Ca-i (h.h)	13.43 ± 0.13	14.07 ± 0.16

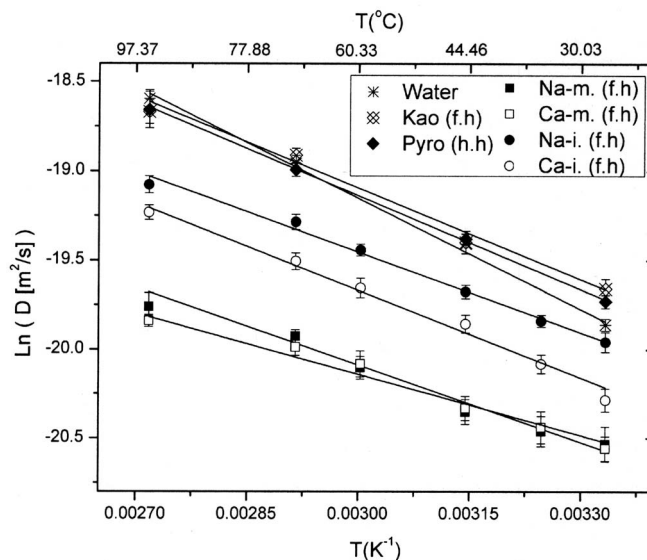


FIG. 6. Arrhenius plot showing the linear temperature dependence of the clay diffusion coefficients and water for the data fitted by the Singwi-Sjölander model.

character than Na^+). Therefore, closer values to that of bulk water were obtained in this case. The above interpretation seems to be reasonable with our observations but other reasons cannot be discarded. The E_a of kaolinite is approximately 15% lower than that of bulk water. Results of NMR measurements^{56,57} showed a reduction in the rotational activation energy of water in contact with kaolinite surfaces. This was explained by reduced or weaker H-bonds between the water and the clay, which is in agreement with the interpretation of the translational E_a data obtained in our study.

Half-hydrated pyrophyllite showed results similar to kaolinite. Interestingly kaolinite and pyrophyllite (uncharged clays with partly hydrophobic character) have larger E_a than both montmorillonites but still lower than that of bulk water. Thus, the increase in diffusion due to the presence of hydrophobic surfaces disappears at higher temperatures, at which both clays have a more waterlike behavior. In our opinion it reminds us unclearly how much this hydrophobicity affects the E_a results.

The activation energy for the half-saturated Ca-illite is lower than that for the fully-saturated sample. In this clay the water seemed to be more influenced by the clay surfaces (decrease E_a) than by the cations (increase E_a), such that the proposed weakening of the H-bonds seems to become more relevant. In the same way, but for montmorillonite, Malikova *et al.*²⁸ found by molecular modeling values of 12–15 kJ/mol for the monohydrated montmorillonite (Cs- and Na-form) and higher values for the bihydrated Na-montmorillonite with 14–19 kJ/mol. Experimental values of bihydrated Ca-montmorillonite samples were found to be in the same range as ours with $E_a = 11 \pm 1$ kJ/mol.¹¹ No data regarding the activation energy were found for illite or uncharged clays.

V. SUMMARY AND CONCLUSIONS

Diffusion of water in highly compacted clays could be successfully quantified by QENS studies. The measurements performed at three different wavelengths showed good agreement, which increases the confidence in the parameters obtained. The two jump diffusion models used to fit the translational diffusion parameters (Singwi–Sjölander and Hall–Ross) described the data very accurately but gave slightly different results. The former makes it impossible to decide which model is more appropriate. Possibly for charged clays different jump length distributions could be applied; in this case average values from both models may be used.

The differences in the clay structures were reflected in the diffusive properties of the confined water. Charged clays had lower diffusion coefficients D and larger residence times τ_r , mean jump lengths l , and rotational relaxation times τ_r than uncharged clays. Within charged clays, Na- and Ca-montmorillonite were found to reduce the water diffusion stronger due to their particular confining interlayer structure. The diffusive parameters for the compacted montmorillonite pellets studied here are similar to those previously found clay powders^{11,16} at the same level of hydration. Both montmorillonites showed similar diffusion results probably because the

water motion is dominated by the interlayer confinement rather than by the difference in the saturating cation (Na^+ or Ca^{2+}) for the particular bilayer hydration studied. However, when the cations are located predominantly on the external surfaces, as in the case of the two types of illite, the behavior of the water motion is affected differently depending on the type of cation. Ca^{2+} reduces the water mobility stronger than Na^+ , as also occurs in aqueous solutions. Uncharged clays had a more waterlike behavior (sometimes even larger diffusion coefficients than bulk water) possibly due to their hydrophobic character. Kaolinite showed larger values in τ_r and l than water, which is attributed to the contribution of the hydrophilic octahedra layer.

Charged clays at reduced water contents showed a further reduction in the effective diffusion coefficients and an increase in τ_l and τ_r . This is indicative of the stronger interaction between the water and the clay surfaces and cations. Dehydration caused no effect on the l values for all the clays. Na-montmorillonite at even lower water contents (q.h) showed no appreciable differences with respect to the h.h samples. The number of water layers for the h.h clay is already so low that a further reduction in the water content did not affect the diffusivity. These results confirm that the cations have only a minor effect on the diffusion of water as compared with the clay surfaces due to the reduced confinement. Uncharged clays at a half water saturation showed no differences in the diffusion parameters as compared with the f.h samples due to the large amount of free pore water still present in these systems.

Fully-water-saturated charged and uncharged clays had lower activation energy values than bulk water. We think that the interaction of water with the clay surfaces may weaken and distort the H-bonds of the water molecules and thus decrease E_a . The disturbance of the H bonds due to surface interactions was observed especially in the case of the two montmorillonites (water distributed in the reduced interlayer confinement) which had the lowest E_a values, which confirms our hypothesis. The activation energy for charged clays was found to be lower than or equal to that for the uncharged clays. The kosmotrope character of the cations was not reflected in the activation energy values of montmorillonites but in the illites, having a larger E_a for the Ca-form than for the Na-form. Ca-illite at a reduced water content (h.h.) showed a lower E_a than the f.h form. This is attributed to the suggested weakening of the H-bonds, since the water molecules at this hydration rate seem to be more influenced by the clay surfaces than by the cations. Hydrophobic surfaces such as those of kaolinite and pyrophyllite were also found to reduce E_a .

ACKNOWLEDGMENTS

The authors would like to thank to G. Kosakowski for help in programming and discussions concerning the 2D analysis and B. Baeyens for many helpful discussions. The DAVE package software is acknowledged (<http://www.ncnr.nist.gov/dave/>) for the data analysis. This work is based on experiments performed at the Swiss spallation neu-

tron source SINQ, Paul Scherrer Institute, Villigen, Switzerland and FRM II, Garching, Germany.

- ¹M. Weik, U. Lehnert, and G. Zaccai, *Biophys. J.* **89**, 3639 (2005).
- ²N. T. Skipper, P. A. Lock, J. O. Titiloye, J. Swenson, Z. A. Mirza, W. S. Howells, and F. Fernandez-Alonso, *Chem. Geol.* **230**, 182 (2006).
- ³S. H. Park and G. Sposito, *J. Phys. Chem. B* **104**, 4642 (2000).
- ⁴V. Marry and P. Turq, *J. Phys. Chem. B* **107**, 1832 (2003).
- ⁵D. Chakrabarty, S. Gautam, S. Mitra, A. Gil, M. A. Vicente, and R. Mukhopadhyay, *Chem. Phys. Lett.* **426**, 296 (2006).
- ⁶J. Swenson, R. Bergman, and S. Longeville, *J. Chem. Phys.* **121**, 9193 (2004).
- ⁷P. Porion, M. Al-Mukhtar, A. M. Faugere, and A. Delville, *J. Phys. Chem. B* **108**, 10825 (2004).
- ⁸Y. Nakashima, *Am. Mineral.* **86**, 132 (2001).
- ⁹G. Vasseur, I. Djeranmaigre, D. Grunberger, G. Rousset, D. Tessier, and B. Velde, *Mar. Pet. Geol.* **12**, 941 (1995).
- ¹⁰D. J. Cebula, R. K. Thomas, and J. W. White, *Clays Clay Miner.* **29**, 241 (1981).
- ¹¹J. J. Tuck, P. L. Hall, M. H. B. Hayes, D. K. Ross, and C. Poinignon, *J. Chem. Soc., Faraday Trans. 1* **80**, 309 (1984).
- ¹²N. Malikova, A. Cadene, V. Marry, E. Dubois, P. Turq, M. Zanotti, and S. Longeville, *J. Chem. Phys.* **317**, 226 (2005).
- ¹³J. Swenson, R. Bergman, and W. S. Howells, *J. Chem. Phys.* **113**, 2873 (2000).
- ¹⁴H. Ohtaki and T. Radnai, *Chem. Rev. (Washington, D.C.)* **93**, 1157 (1993).
- ¹⁵H. van Olphen, *An Introduction to Clay Colloid Chemistry: For Clay Technologists, Geologists, and Soil Scientists* (John Wiley & Sons, New York, 1977) 2nd, Ed.
- ¹⁶N. Malikova, A. Cadene, V. Marry, E. Dubois, and P. Turq, *J. Phys. Chem. B* **110**, 3206 (2006).
- ¹⁷M. A. Anderson, F. R. Trouw, and C. N. Tam, *Clays Clay Miner.* **47**, 28 (1999).
- ¹⁸C. H. Bridgeman, A. D. Buckingham, N. T. Skipper, and M. C. Payne, *Mol. Phys.* **89**, 879 (1996).
- ¹⁹S. V. Churakov, *J. Phys. Chem. B* **110**, 4135 (2006).
- ²⁰C. H. Bridgeman and N. T. Skipper, *J. Phys.: Condens. Matter* **9**, 4081 (1997).
- ²¹J. Hartnig, W. Witschel, and E. Spohr, *J. Phys. Chem. B* **102**, 1241 (1998).
- ²²I. Brovchenko, A. Geiger, A. Oleinikova, and D. Paschek, *Eur. Phys. J. E* **12**, 69 (2003).
- ²³M. R. Warne, N. L. Allan, and T. Cosgrove, *Phys. Chem. Chem. Phys.* **2**, 3663 (2000).
- ²⁴D. Tunega, L. Benco, G. Haberhauer, M. H. Gerzabek, and H. Lischka, *J. Phys. Chem. B* **106**, 11515 (2002).
- ²⁵D. Tunega, G. Haberhauer, M. H. Gerzabek, and H. Lischka, *Langmuir* **18**, 139 (2002).
- ²⁶B. Hribar, N. T. Southall, V. Vlachy, and K. A. Dill, *J. Am. Chem. Soc.* **124**, 12302 (2002).
- ²⁷P. S. Leung and G. J. Safford, *J. Phys. Chem.* **74**, 3696 (1970).
- ²⁸N. Malikova, V. Marry, J. F. Dufreche, C. Simon, P. Turq, and E. Giffaut, *Mol. Phys.* **102**, 1965 (2004).
- ²⁹*Bentonite der Insel Milos, Griechenland*, edited by A. Decher (T.H., Aachen Germany, 1997).
- ³⁰V. Gabis, *Bull. Soc. Fr. Mineral. Cristallogr.* **81**, 183 (1958).
- ³¹H. van Olphen and J. J. Fripiat, *Data Hand Book for Clay Minerals* (Pergamon, Oxford, 1979).
- ³²F. González Sánchez, L. Van Loon, T. Gimmi, A. Jakob, and M. Glaus, *Appl. Geochem.* <http://dx.doi.org/10.1016/j.apgeochem.2008.08.008>
- ³³B. Baeyens, personal communication (Feb. 2007).
- ³⁴A. M. Scheidegger, G. M. Lamble, and D. L. Sparks, *Environ. Sci. Technol.* **30**, 548 (1996).
- ³⁵T. Kozaki, A. Fujishima, S. Sato, and H. Ohashi, *Nucl. Technol.* **121**, 63 (1998).
- ³⁶R. Pusch, Technical Report No. TR-01-08, 2001.
- ³⁷R. A. Schwarzer, *Texture mapping by scanning X-ray diffraction and related methods*. In: *Advanced X-Ray Techniques in Research and Industry*. Edited by A. K. Singh (IOS Press, Amsterdam, The Netherlands, 2005) pp. 50–65.
- ³⁸S. Janssen, J. Mesot, L. Holitzner, A. Furrer, and R. Hempelmann, *Physica B* **234**, 1174 (1997).
- ³⁹T. Unruh, J. Neuhaus, and W. Petry, *Nucl. Instrum. Methods Phys. Res. A* **580**, 1414 (2007).
- ⁴⁰S. H. Chen, P. Gallo, F. Sciortino, and P. Tartaglia, *Phys. Rev. E* **56**, 4231 (1997).
- ⁴¹M. Bee, *Quasielastic Neutron Scattering: Principles and Applications in Solid State Chemistry, Biology and Material Science*, edited by Adam Hilger (IOP, Bristol, 1988).
- ⁴²P. L. Hall and D. K. Ross, *Mol. Phys.* **42**, 673 (1981).
- ⁴³K. S. Singwi and A. Sjolander, *Phys. Rev.* **119**, 863 (1960).
- ⁴⁴J. Swenson, R. Bergman, D. T. Bowron, and S. Longeville, *Philos. Mag. B* **82**, 497 (2002).
- ⁴⁵V. F. Sears, *Can. J. Phys.* **44**, 1299 (1966).
- ⁴⁶E. Mamontov, *Can. J. Phys.* **121**, 9087 (2004).
- ⁴⁷H. N. Bordallo, L. P. Aldridge, and A. Desmedt, *J. Phys. Chem. B* **110**, 17966 (2006).
- ⁴⁸H. R. Pruppacher, *J. Chem. Phys.* **56**, 101 (1972).
- ⁴⁹J. H. Wang, *J. Phys. Chem.* **58**, 686 (1954).
- ⁵⁰N. A. Hewish, J. E. Enderby, and W. S. Howells, *J. Phys. C* **16**, 1777 (1983).
- ⁵¹G. Sposito and R. Prost, *Chem. Rev. (Washington, D.C.)* **82**, 553 (1982).
- ⁵²J. Teixeira, M. C. Bellissentfunel, S. H. Chen, and A. J. Dianoux, *Phys. Rev. A* **31**, 1913 (1985).
- ⁵³R. E. Lechner, *Solid State Ionics* **77**, 280 (1995).
- ⁵⁴P. F. Low, *Clays Clay Miner.* **9**, 219 (1962).
- ⁵⁵J. H. Wang, *J. Am. Chem. Soc.* **73**, 510 (1951).
- ⁵⁶J. J. Fripiat, M. Letellier, and P. Levitz, *Philos. Trans. R. Soc. London, Ser. A* **311**, 287 (1984).
- ⁵⁷J. Jonas, D. Brown, and J. J. Fripiat, *J. Colloid Interface Sci.* **89**, 374 (1982).